

Characterization of an Annular Helicon Plasma Source

IEPC-2007-202

*Presented at the 30th International Electric Propulsion Conference, Florence, Italy
September 17-20, 2007*

Douglas Palmer,^{*} Cengiz Akinli,[†] Logan Williams,[‡] and Mitchell L. R. Walker II[§]
High-Power Electric Propulsion Laboratory, Georgia Institute of Technology, Atlanta, GA, 30332, USA

Abstract: The Georgia Institute of Technology (GA Tech) has created a nominally 1-kW annular helicon plasma source that is sized to interface with a 5-kW Hall effect thruster. The electron number density and electron temperature of the plasma are measured with an RF-compensated Langmuir probe as a function of axial and radial location within the plasma column, and RF forward power (100 W- 1.0 kW). All tests are performed in the GA Tech Vacuum Test Facility. Measurements show the plasma source produces electron temperatures from 16.9 eV to 19.25 eV, and electron number densities from $1.2 \times 10^{12} \text{ cm}^{-3}$ to $7.2 \times 10^{13} \text{ cm}^{-3}$ at a point 519 mm downstream of the propellant distributor.

Nomenclature

A_c	=	plasma column cross-sectional area
A_p	=	Langmuir probe collection area
e	=	electron charge
GCF	=	gas correction factor
HET	=	Hall effect thruster
I_{es}	=	electron saturation current
k	=	Boltzmann constant
m	=	azimuthal wave mode
m_e	=	electron mass
n_e	=	electron number density
n_i	=	ion number density
n_n	=	neutral number density
n_o	=	equilibrium plasma density
OML	=	Orbital Motion Limited
P	=	chamber pressure
P_b	=	base pressure,
P_{ob}	=	observed chamber pressure with propellant mass flow
r	=	radial distance from annular helicon centerline
r_p	=	Langmuir probe collector radius
T_e	=	electron temperature
VTF	=	Vacuum Test Facility
V_D	=	discharge voltage
V_{nc}	=	neutralizer coupling voltage
V_f	=	plasma floating potential

^{*} Graduate Student Researcher, Aerospace Engineering, dougpalmer@gatech.edu.

[†] Graduate Student Researcher, Aerospace Engineering, cakinli@gatech.edu

[‡] Graduate Student Researcher, Aerospace Engineering, gtg775r@mail.gatech.edu

[§] Assistant Professor, Aerospace Engineering, mitchell.walker@ae.gatech.edu

x	=	axial displacement from annular helicon anode
ε	=	ionization cost
λ_D	=	Debye length
γ	=	plume divergence coefficient
η	=	propellant ionization efficiency
μ_0	=	permeability of free space
ν	=	collision rate

I. Introduction

The United States Air Force (USAF) requires a Hall effect thruster (HET) that operates at low specific impulses and high thrust-to-power (T/P) ratios. To date, the performance goal remains unsatisfied by standard HET configurations. This is primarily due to the inefficiency of the DC electron bombardment ionization process of the HET. The Georgia Institute of Technology High-Power Electric Propulsion Laboratory (HPEPL) research program seeks to develop and understand a high-density, high-efficiency (~80-90%) annular helicon plasma source and incorporate it into an HET.

Helicon plasma sources sustain steady-state plasma production through absorption and propagation of helicon waves.¹ Helicon waves are launched by applying an axial magnetic field and coupling an RF antenna to the plasma column.² This process is much more efficient and can provide plasma densities an order of magnitude greater than previous inductive methods for the same input power.³ Currently, helicon plasma sources only exist in cylindrical configurations, which is not optimal for some applications. Yano and Walker have shown that it is feasible to produce helicon plasmas in an annular geometry.⁴ An annular helicon theoretical model has been developed and trade studies have been performed, indicating the plasma number densities required by a two-stage HET are attainable.² A high density, high efficiency annular helicon requires dual concentric left-helical antennas to theoretically excite the helicon ($m=1$) mode within the annulus, however experimental verification of helicon wave mode has not been established. HPEPL has designed, built, and operated this device, creating plasmas of unknown power coupling throughout the 7 – 15 MHz frequency range and 0 – 450 Gauss range. Previous works have indicated the wave mode can be identified by jumps in ion saturation current.⁵ This research effort characterizes the plasma source as a function of axial and radial location, RF forward power, and attempts to verify the mode of the plasma being produced (*i.e.*, inductively coupled or Helicon wave mode).

II. Experimental Apparatus

A. Facility

All experiments are performed in the Vacuum Test Facility (VTF), shown schematically in Fig. 1. The VTF is a stainless steel vacuum chamber that has a diameter of 4 m and a length of 7 m. Two 3800 CFM blowers and two 495 CFM rotary-vane pumps evacuate the facility to moderate vacuum (30 mTorr). To reach high-vacuum (10^{-7} Torr), the VTF employs six 48" diffusion pumps, with a combined nominal pumping speed of 600,000 l/s on air, 840,000 L/s on hydrogen, and 155,000 l/s on xenon. The VTF pumping speed is varied by changing the number of diffusion pumps in operation. The combined pumping speed of the facility is 600,000 l/s on air and with a base pressure of 9.9×10^{-4} Pa (7.5×10^{-6} Torr).

Table 1 shows the VTF operating pressure for each flow rate. Previous investigations show these pressures are adequate for plume and performance measurements.⁶ The chamber pressures listed in are the indicated pressures from the ionization gauge, corrected for argon using the known base pressure on air and a gas correction factor (GCF) of 1.20.

$$P = \frac{P_{ob} - P_b}{GCF} + P_b \quad (1)$$

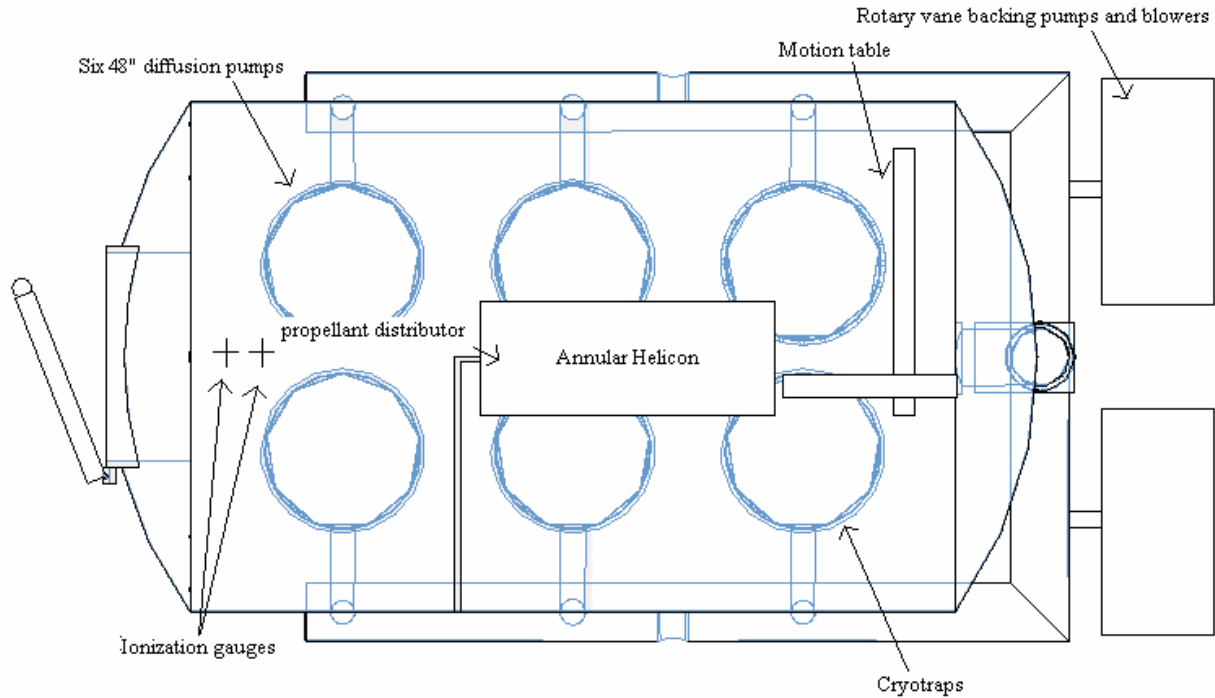


Figure 1. Schematic of Vacuum Test Facility. As viewed from above.

The gauge is a Varian model UHV-24 ionization gauge with a KJLC model IG2200 vacuum gauge controller. The UHV-24 ionization gauge is calibrated for air by the manufacturer. The ionization gauge measures pressure over the range of 10^{-2} Pa (10^{-4} Torr) to 10^{-10} Pa (10^{-12} Torr) with an accuracy of $\pm 20\%$ as reported by Varian.⁷ The VTF also utilizes a tabulated KJLC model G100TF ionization gauge with a KJLC model IG2200 ionization gauge controller, and a KJLC Accu-Quad residual gas analyzer, both located on the top of the chamber.

Mass flow rate, sccm Ar	Mass flow rate, mg/s	Operating Pressure, Torr-Ar
25	0.74	1.2E-05
50	1.48	1.3E-05
75	2.22	1.7E-05
100	2.97	1.9E-05

Table 1. Operating pressures for mass flow rates of argon.

B. Annular Helicon Plasma Source

All experiments are performed on the annular helicon plasma source shown in Fig. 2. A schematic of the annular helicon RF power, solenoid, and mass flow systems is shown in Fig. 3. The annular glass channel is comprised of two concentric 6 mm thick Pyrex tubes with outer diameters of 120 mm and 178 mm, respectively. Copper inner and outer helical pitch antennas are wrapped on both the inner and outer tube. The power leads to the antennas as well as the solenoids are EMF shielded with tinned copper mesh to eliminate RF radiation. The antennas can be wired with the same or opposite current directions, and are set such that the legs twist are on top of one another, which allows for the best coupling of the antennas to the plasma.²

Five solenoids generate steady-state axial magnetic fields of up to 450 Gauss, and are powered by a 60-kW EMHP DC power supply. High purity (99.9995% pure) argon gas is fed through an MKS 1179JA mass flow

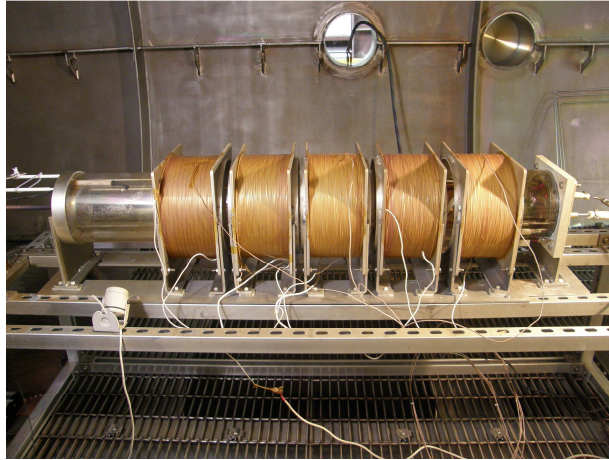


Figure 2. Annular helicon plasma source.

controller through stainless steel feed lines to the anode. A fully customized calibration system is employed to calibrate the mass flow controller. The mass flow controller has an accuracy of $\pm 1\%$.

C. Langmuir Probe Theory

Electron number density and temperature measurements are taken with an RF-compensated Langmuir probe. RF-compensated Langmuir probes have been extensively researched in the work of Sudit and Chen, and if properly compensated have proven to be accurate for measuring plasma characteristics even in the presence of magnetic fields below 350 Gauss.⁸ Orbital Motion Limited (OML) theory may be used to calculate the plasma parameters for a small ratio of probe radius to Debye length, eliminating any absorption radius.⁹

$$r_p / \lambda_D \ll 3 \quad (2)$$

OML theory uses the fact that ion collection current is independent of the shape of the plasma potential, assuming the current is only limited by the angular momentum of the ions about the probe, and that there exists a sheath edge outside of which the energy distribution is Maxwellian. A schematic of the OML sheath and an absorption boundary is shown in Fig. 5. Probes of this size can be analyzed by other theories; however, Chen recommends construction of thin probes so that OML theory may be used,⁹ which provides a simple relationship for ion current, in Eqn. (3).

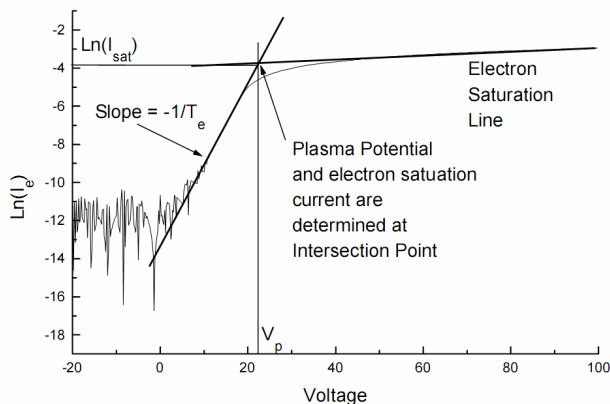


Figure 4. Natural Logarithm of current versus bias voltage of a Langmuir probe.¹⁰

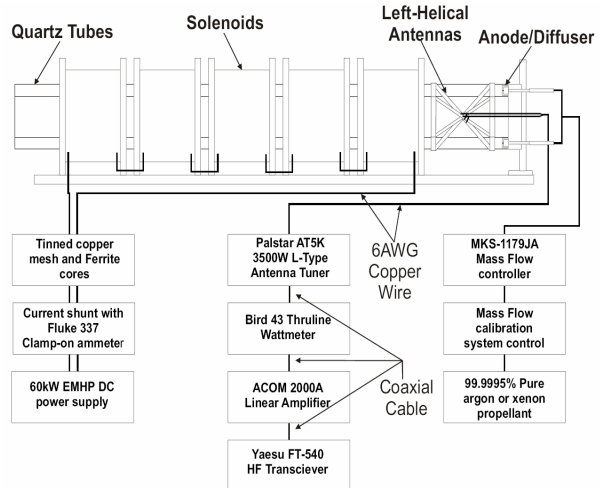


Figure 3. Schematic of Annular Helicon subsystems. RF Power, magnetic solenoids, and mass flow systems.

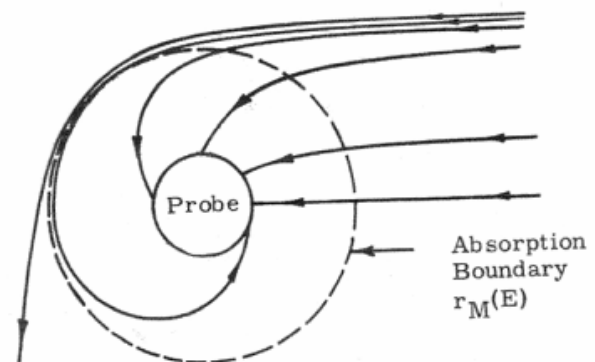


Figure 5. OML theory electron motion near a positively-biased Langmuir probe.⁹

$$I \xrightarrow{T_i \rightarrow 0} A_p n_e \frac{\sqrt{2}}{\pi} \left(\frac{|eV_p|}{M} \right)^{1/2} \quad (3)$$

To analyze the raw I-V data, the square root of the ion current fit is added to the original I-V curve to obtain a characteristic, which consists of electron current only. The natural logarithm of the electron current is calculated and plotted against the bias voltage. The electron temperature and electron number density are calculated by fitting a line to the linear transition region as shown in Fig. 4. The relationships for electron temperature and electron number density are shown in Eqs (4) and (5).¹⁰

$$T_e = \frac{-1}{slope_{\ln(I)}} \quad (4)$$

$$n_e = 3.73 \times 10^{13} \frac{I_{es(amps)}}{A_p(m^2) \sqrt{T_e(eV)}} \quad (5)$$

D. Probe Construction and Circuit

Two RF-compensated Langmuir probes are constructed for this experiment based upon the Chen B probe design⁹ and are shown schematically in Fig 6. The probes are identical, except the collection tip is parallel to the probe body axis in one case and perpendicular in the other. This allows for higher resolution in both axial and radial measurements, as the probe may be oriented entirely along the axis where the measurement is desired. This is necessary for radial profiles, where the annular helicon channel width is only 29 mm. The RF compensation electrode is large compared to the probe radius, improving probe accuracy.⁹ Self-resonating RF-chokes are required to achieve the necessary impedances at the operating frequencies, and were selected based on the requirements set forth by Sudit and Chen.⁸

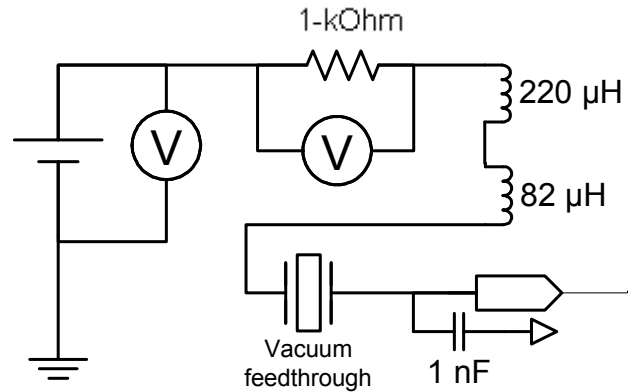


Figure 6. Wiring Schematic for RF-compensated Langmuir probes.

The probe consists of a 0.005” diameter tungsten electrode, 0.005” thickness nickel foil compensation electrode, and 1000 pF capacitor. The probe lead attaches to a 1-kΩ resistor and terminates at the chamber ground. A LabView VI reads the probe voltage and calculates the probe current from the voltage drop across the resistor. A Keithley 2410 Sourcemeter supplies the probe bias, with the voltage across the resistor measured by an Agilent 34970A Data Acquisition Unit. The probe is mounted to a 1.5 m by 1.5 m Parker Daedel automated motion control system to provide linear axial and radial motion with an accuracy of $\pm 1 \mu\text{m}$.

E. Probe Verification

To verify the accuracy of the probe setup, electron number density and electron temperature measurements are conducted on DC plasma produced by the Electric Propulsion Lab (EPL) model HCPEE 375 hollow cathode electron emitter. EPL documentation lists typical electron temperatures of 1 – 2 eV for this device. The resulting curves are expected to coincide with ideal OML I-V curves for DC plasma, as shown in Figs. 7 and 8. Data analysis on the hollow cathode plasma indicates an electron temperature of 1.9 eV, which falls within the range of the capabilities of the device.

In this experiment, the only difference between the measurements and ideal I-V curves is the significantly lower operating pressure of the VTF (9.1×10^{-6} Torr). This data indicates that the increased slope of the electron saturation region may be attributable to this decreased chamber pressure.⁹ Increased slope in the electron saturation region is also seen in future RF-compensated Langmuir probe measurements taken for the annular helicon.

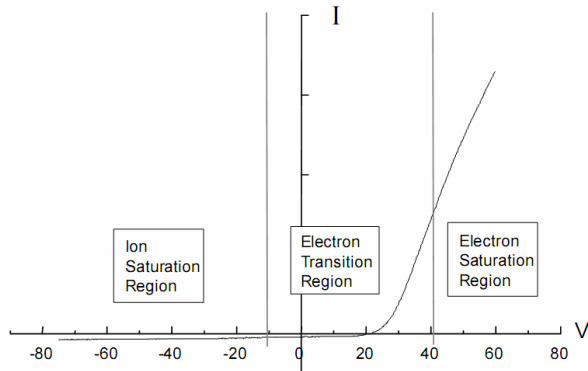


Figure 7. Typical I-V characteristic applicable to OML theory analysis.¹⁰

While performing measurements on the annular helicon plasma source, the probe must be traversed into the plasma channel. It is necessary to illustrate the plasma is not significantly affected by the probe. The probe was manufactured to have a much smaller tip and shaft diameter than the channel width, which minimizes measurement intrusion on the plasma.⁸ A B-dot probe is used to measure the effective change in the perturbed magnetic field during traverses of both probes one at a time, each during biased and unbiased probe measurements. The B-dot probe consists of five turns of no. 18 solid copper wire, in a 0.125" diameter loop. The B-dot probe is located 600 mm downstream of the anode, and the coil axis is oriented parallel to the helicon axis.

Multiple B-dot measurements are taken at each axial location. Fig. 9 shows that there is no significant effect upon the plasma from traversing either the straight or bent probe, both during measurements or in-between samples, as there is no significant trend in the data as the probe is traversed. The range of values in the data was $\pm 2\%$ of the mean, which is well within the B-dot probe data error limits. Examples of the B-dot time-resolved data sweeps are shown in Fig. 10. The peak and minimum amplitude at each cycle is used to determine trends within the trace, as well as average difference in total amplitudes. While minimal differences are observed, the overall trend is constant. Lastly, it is necessary to verify the inductor chokes are tuned properly to the applied RF frequency (13.56 MHz). Figure 11 shows the impedance-frequency relationship for both the two inductor and four inductor chokes used in experiments. These curves indicate that while the peak impedance value is located slightly below the applied frequency, the chokes still exhibit acceptable impedance to the

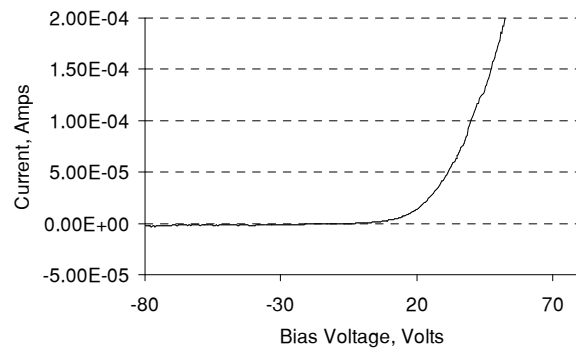


Figure 8. I-V characteristic for an EPL 375 series hollow cathode. 10 A, 2 sccm xenon.

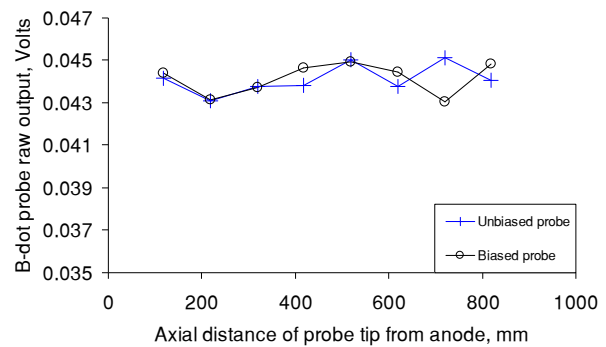


Figure 9. B-dot probe raw output versus axial distance of probe tip from anode. 13.56 MHz RF frequency, 350 G Magnetic field, 2.97 mg/s argon.

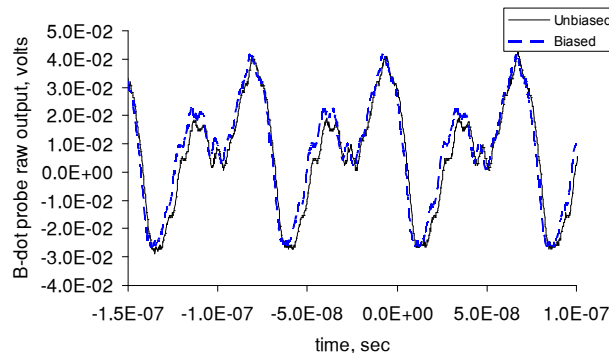


Figure 10. B-dot probe time resolved raw data output for unbiased probe traverse.

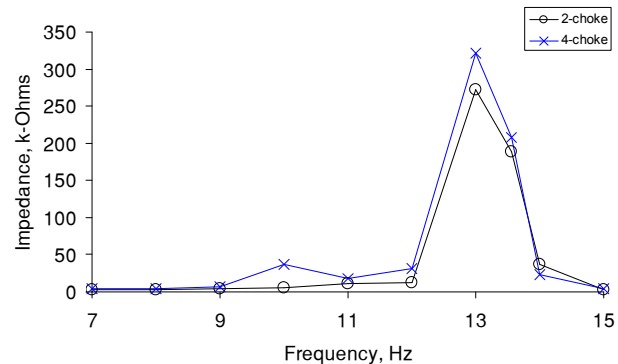


Figure 11. Impedance versus frequency relationship for 2-inductor and 4-inductor chokes used.

load at the operating condition.⁸ However, inductors could be screened and chosen to resonate to higher impedances at the operating frequency, since Sudit and Chen have shown that 1 M Ω impedance is attainable from a single choke.⁸

III. Experimental Results

This experiment consists of three sections, which determine the location of the peak plasma number density and electron temperature as a function of axial and radial location, as well as RF forward power. A radial profile is first taken to determine the peak plasma density location within the channel radius, followed by an axial profile along centerline determining the peak values along the axis of the device. RF forward power profiles are then taken at 519 mm downstream of the antenna long channel centerline. The peak electron temperature and electron number density is measured at a location 519 mm downstream of the antenna on channel centerline. The RF power profile may indicate the existence of helicon mode within the plasma.⁵

Each data section is taken for two configurations of the annular helicon. Yano has concluded that the ‘driven’ RF leads on the inner and outer antennas should be inverted, *i.e.*, current flows towards the discharge end of the annular helicon on the outer antenna, and away from it on the inner antenna.² However, it has been experimentally verified that antenna-plasma coupling can be achieved in both antenna current configurations. Both setups are characterized in this analysis. For all operating conditions, the standing wave ratio is nearly zero. With less than 5 W reflected power at 13.56 MHz, indefinite steady-state operation can be achieved at 500 W RF forward power. The RF forward and reflected power are measured with the internal meter on the matching network. Measured data points are connected in the following section for reader clarity.

F. Radial profile

The body-aligned RF-compensated Langmuir probe is used to take a radial profile of the electron temperature and electron number density. This probe allows for a 0.005” radial resolution if necessary. I-V curves are taken and analyzed with OML theory as discussed above.

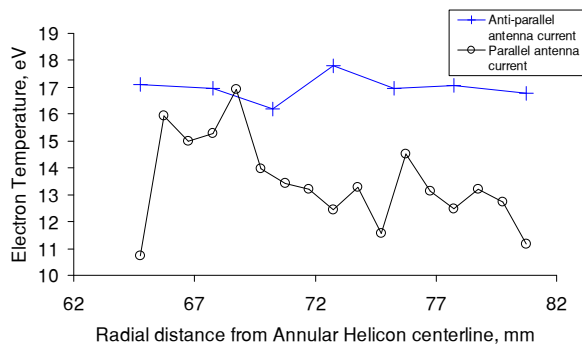


Figure 12. Electron temperature versus distance from Annular helicon centerline. 13.56 MHz RF frequency, 1 kW RF forward power, < 5 W reflected, 350 G magnetic field, 2.97 mg/s argon, operating pressure 1.9×10^{-5} Torr-Ar, 200 mm downstream of antennas. The center of the plasma channel is at 72.75 mm.

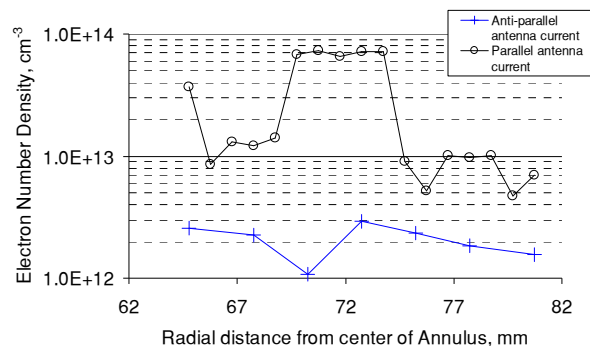


Figure 13. Electron number density versus distance from Annular helicon centerline. 13.56 MHz RF frequency, 1 kW RF forward power, < 5 W reflected, 350 G Magnetic field, 2.97 mg/s argon, operating pressure 1.9×10^{-5} Torr-Ar, 200 mm downstream of antennas. The center of the plasma channel is at 72.75 mm.

Figure 12 shows the anti-parallel antenna current configuration yields the highest temperatures, ranging from 16.21 eV to 17.81 eV. While a peak is seen in the center of the channel, overall the trend is flat across the channel width. Parallel antenna current shows a peak in electron temperature at 62.25 mm from the annulus centerline. While the parallel antenna current configuration seems to show a positive trend moving towards device centerline, the change is still within the error bounds of the theory. However, repeatability studies indicate a similar trend.

Figure 13 shows that electron number density for the anti-parallel current configuration exhibits the same behavior as its electron temperature counterpart. While a peak of $2.9 \times 10^{12} \text{ cm}^{-3}$ exists near the channel centerline, the overall trend is mostly flat. In the parallel antenna current cases, higher electron number densities are reached, with a peak value of $7.2 \times 10^{13} \text{ cm}^{-3}$. The plasma density decreases sharply towards the channel walls, which may

prove more useful when attempting to use the annular helicon as a preionization stage for a Hall effect thruster.² The trends seen in the parallel current case are well outside the $\pm 30\%$ error limits, and can be correlated to the theoretical model for an annular helicon.¹¹

G. Axial profile

The perpendicular RF-compensated Langmuir probe is used to determine the axial variation of electron temperature and electron number density in the device. I-V curves are taken along the plasma channel centerline, which is the maximum electron temperature location as determined by the peak in the radial profile. The antennas end at 490 mm, and the magnetic solenoids span from 50 mm to 850 mm. The variation in electron temperature is shown below.

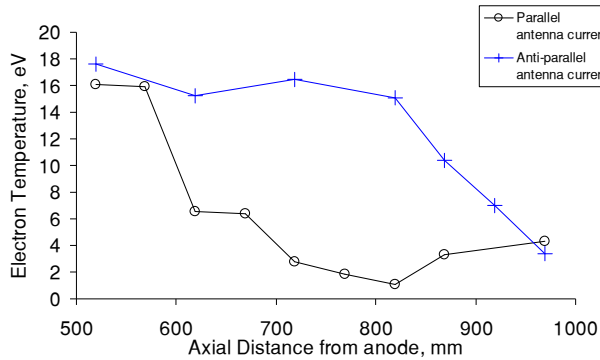


Figure 14. Electron temperature versus axial distance from propellant diffuser. 13.56 MHz RF frequency, 1 kW RF forward power, < 5 W reflected, 350 G Magnetic field, 2.97 mg/s argon, operating pressure 1.9×10^{-5} Torr-Ar, channel centerline.

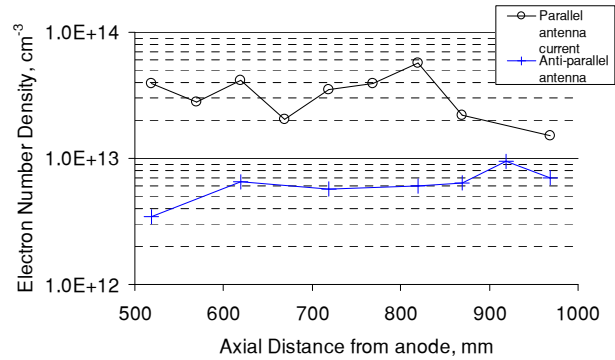


Figure 15. Electron number density versus axial distance from propellant diffuser. 13.56 MHz RF frequency, 1 kW RF forward power, < 5 W reflected, 350 G Magnetic field, 2.97 mg/s argon, operating pressure 1.9×10^{-5} Torr-Ar, channel centerline.

Figure 14 illustrates that the anti-parallel current configuration indicates a flat electron temperature in the 15 - 17 eV range, decreasing sharply after the magnetic field lines diverge behind the solenoids at 850 mm. The parallel current case decreases sharply just downstream of the antenna, and stays in the 1.5 – 6.5 eV range down the device.

Figure 15 indicates nearly an order of magnitude increased electron number density for the parallel antenna current case, similar to the radial profiles taken above. The anti-parallel antenna current case indicates a relatively flat profile as before, in the $3 - 9 \times 10^{12} \text{ cm}^{-3}$ range. The parallel antenna current case peaks at $5.6 \times 10^{13} \text{ cm}^{-3}$, and remains relatively constant until passing the end of the magnetic coils.

H. RF power profile

The axial and radial electron temperature and electron number density profiles indicate that the peak plasma parameters may exist 519 mm downstream of the anode, which is the location for investigation of wave modes.⁵ In Fig. 16, the anti-parallel antenna current case exhibits a more varied electron temperature as RF forward power increases. The electron temperature is nearly constant after approximately 600 W. Below 220 W, there is insufficient power to excite a self-sustaining plasma mode. This suggests antenna-plasma coupling is more difficult to establish for the anti-parallel current configuration at this operating condition. The correlation between inductively-coupled and helicon wave modes as a function of power has been examined for this setup.¹¹ The parallel antenna configuration produces a self-sustaining plasma as low as 100 W and quickly reaches its peak electron temperature at 250 W, after which the trend is approximately constant.

The anti-parallel current case shown in Fig. 17 follows a similar trend in electron number density as electron temperature. Self-sustaining plasma is not produced until 300 W, after which coupling is poor relative to the parallel antenna current case. Peak electron number densities are an order of magnitude lower than the parallel case, and do not change significantly with increases in RF power after 500 W. The parallel current case indicates sufficient coupling even at 100 W RF forward power. The maximum electron temperature is measured at 500 W, after which no significant increase in electron number density is observed as the RF power increases.

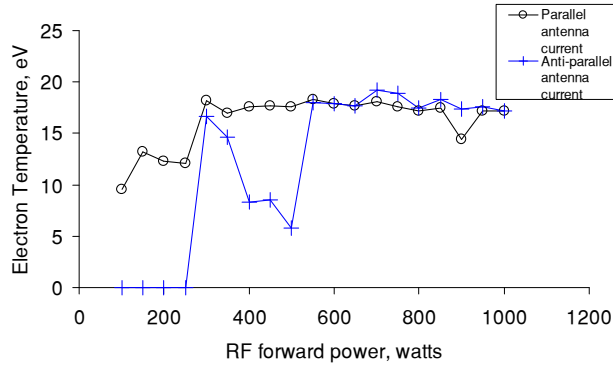


Figure 16 Electron temperature versus RF forward power. 13.56 MHz RF frequency, 519 mm from propellant diffuser, 350 G Magnetic field, 2.97 mg/s argon, operating pressure 1.9×10^{-5} Torr-Ar, channel centerline.

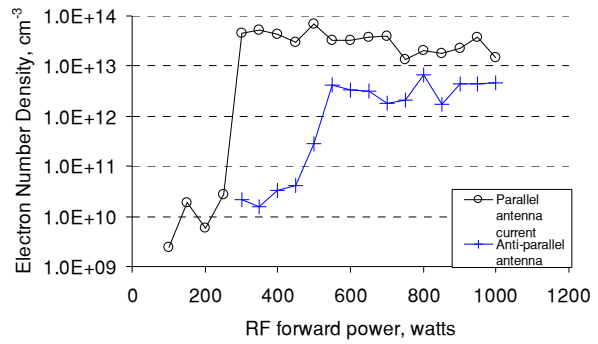


Figure 17. Electron number density versus RF forward power. 13.56 MHz RF frequency, 519 mm from propellant diffuser, 350 G Magnetic field, 2.97 mg/s argon, operating pressure 1.9×10^{-5} Torr-Ar channel centerline.

IV. Discussion

The difficulties of making accurate measurement of the parameters of an RF plasma with Langmuir probe diagnostics are well known.⁸ A number of different approaches have been explored in various attempts to compensate for RF fluctuations in probe currents with varying levels of success.¹¹ Efforts are made to compensate for these fluctuations using some of the approaches detailed in the literature. Still, we continue to find that some of the measures taken provide only limited corrective effects on data.

Measured data indicates trends in electron temperature and electron number density that correlate with established results.² In each profile, as the electron temperature decreases, the electron number density increases. While these are not solely dependent characteristics, they are related by the inverse square root as shown in Eq. (5). Radial electron temperature and electron number density profiles follow known trends as demonstrated by annular helicon theory.² Additionally, RF power profiles suggest wave mode jumps consistent with previous analyses.⁵ Further investigation of the ion saturation current as a function of applied RF power, as well as perturbed magnetic field characteristics will provide more conclusive results of plasma wave mode.

The resulting electron temperature and electron number density measurements indicate higher than normal levels than exist in most helicons. However, the VTF operating pressure is several orders of magnitude lower than most of the reported measurements and the annular helicon dual-antenna configuration is a new regime for RF-compensated Langmuir probe measurements. The difference in slopes from the transition region to the electron saturation region has been shown to decrease as pressure decreases,⁹ similar to I-V curves in this study. Electron temperature and number density measurements in the presence of large magnetic fields are also known to be troublesome to analyze, as large magnetic fields decrease the relative difference in the slope of the transition to electron saturation regions in the resultant I-V curve. This is because the applied magnetic field constrains the thermal motion of electrons, which can produce substantial anisotropy, which in turn conflicts with some of the assumptions fundamental to OML theory. In typical Langmuir probe measurements in magnetized plasmas, high probe voltages draw current to the probe tip, which depletes the electron population available in the flow tube intersecting the tip.^{8,11} This depletion can cause a significant distortion to the I-V characteristic in the regions most critical to the calculation of electron temperature. When the probe body is aligned with the B-field, depletion of the flow tube could cause the deviation from previously published results. The orientation (for a cylindrical probe) that exacerbates this effect maximally is where the tip is parallel to the applied magnetic field. In this experiment, two probes are used, one parallel and one perpendicular to the applied field.

Additionally, the probe tip diameter is $0.005''$, which for the plasma parameters we expected at the time of experiment design, is adequate to ensure that $\beta < 3$. This means that the OML theory is in fact applicable to the plasma under investigation. However, the unexpectedly high electron temperatures calculated under OML suggests the probe tip is too large, and that OML-based analysis may be invalid for the annular helicon. A commercially

available RF-compensated Langmuir probe system validated by Chen¹² has been acquired and will provide another means of data validation.

V. Conclusion

The peak electron temperature recorded is 19.25 eV, and the peak electron number density of $7.2 \times 10^{13} \text{ cm}^{-3}$, at an operating condition of 519 mm downstream of the antenna, on channel centerline, 1 kW RF power. Peak coupling resulting in maximum electron number density can be achieved at less than the maximum power limits of the experimental equipment, approximately 500 W RF forward power. Anti-parallel antenna current configuration, while predicted to provide the most efficient power coupling to the plasma, producing weaker plasma densities and electron temperatures than the parallel antenna current case. This suggests a highly efficient annular helicon plasma source can operate at lower than nominal power and still achieve superior electron number density levels.

Acknowledgments

The authors wish to thank the Marshall Space Flight Center for supplying the RF power system, Andre Carignan, Scott Elliott, Scott Moseley and James Steinberg of the Georgia Tech Aerospace Engineering Machine Shop for fabrication of hardware. This research is supported by the Air Force Office of Scientific Research grant FA9550-07-1-0137. Dr. Mitat Birkan is the contract monitor.

References

1. Chen, F. F., Plasma Ionization by Helicon Waves. *Plasma Physics and Controlled Fusion* 1991, 33, (4), 339-364.
2. Yano, M., Palmer, D, Williams, L, Walker, M. L. R., Design and Operation of an Annular Helicon Plasma Source. In *43rd Joint Propulsion Conference*, Cincinnati, OH, 2007; Vol. AIAA-2007-5309.
3. Chen, F. F., Helicon Wave Plasma Sources. In *Proceedings of the International Conference on Plasma Physics*, Kiev, USSR, 1987; Vol. 2, p 1378.
4. Yano, M., Walker, M. L. R., Plasma Ionization by Annularly-Bounded Helicon Waves. *Physics of Plasmas* 2006, 13, (6).
5. Chi, K.-K., Sheridan, T E, Boswell, R W, Resonant cavity modes of a bounded helicon discharge. *Plasma sources Sci. Technol.* 1999, 8, 421-431.
6. Randolph, T., Kim, V., Kaufman, H., Kozubsky, K., Zhurin, V. V., Day, M., "Facility Effects on Stationary Plasma Thruster Testing". In *23rd International Electric Propulsion Conference*, Seattle, WA, 1993; Vol. IEPC-93-93.
7. Varian, Vacuum Measurement. In Varian, Inc.: 2003.
8. Sudit, I. D., Chen, F. F., RF compensated probes for high-density discharges. *Plasma Sources Sci. Technology* 1994, 3, (162).
9. Chen, F. F., RF Langmuir Probes, revisited. In *58th Gaseous Electronics Conference*, San Jose, CA, 2005.
10. *Hidden Handbook of Plasma Diagnostics*; Warrington, England.
11. Akinli, C., Palmer, D, Walker, M. L. R., Comparison of the Theoretical and Experimental Performance of an Annular Helicon Plasma Source. In *30th International Electric Propulsion Conference*, Florence, Italy, 2007; Vol. IEPC-2007-236.
12. Chen, F. F., Time-Varying impedance of the sheath on a probe in an RF plasma. *Plasma sources Sci. Technol.* 2006, 15, 773-782.